Numerical studies of neon pellet ablation in tokamaks

N. Bosviel[1], R. Samulyak[1,2], P. B. Parks[3], N. Naithlo[1], S. Yuan[1]

[1] *Stony Brook University, Stony Brook, NY, USA*

[2] *Brookhaven National Laboratory, Upton, NY, USA*

[3] *General Atomics, San Diego, CA, USA*

Impurities injection experiments into magnetic fusion reactors have proven successfull in mitigating plasma disruptions [1]. Previous and on going analytical and semi-analytical studies for single pellet ablation provide valuable insight for penetration studies and a robust physical framework for the simulations presented in this paper. In the present work, we extended capabilities of the code in [2] to simulate neon / high-Z pellets in the plasma disruption mitigation parameter space and improved numerical methods and solvers. The model resolves the solid to gas phase transition, formation of the dense, cold cloud of ablated material, the deposition of energy from hot plasma electrons passing through the ablation cloud, the atomic processes in the cloud, the channel creation along magnetic field lines and the radiation losses. The streaming hot plasma electrons heat flux is represented by an external heat source similar to [7, 2] but updated for neon pellets [4]. Tabular equation of state based on the Saha-LTE model is used for the simulation of atomic processes. The ablation cloud partially shields the pellet from the incoming plasma energy flux and is the main factor controlling the ablation rate. Following [2] where the magnetic Reynold's number $R_m \ll 1$ near the pellet and the magnetic $\beta \ll 1$ in the far field, the magnetic field is taken to be constant and uniform, supporting the electrostatic MHD approximation.

Our hybrid Eulerian-Lagrangian pellet code uses front tracking [3], a numerical method in which a co-dimension 1 Lagrangian mesh (front) follows distinguished waves in the system (such as contact discontinuities) on an Eulerien space-filling mesh, used for the integration of the governing equations. Front tracking preserves and maintains sharp discontinuities by avoiding taking derivatives across interfaces of steep gradients. The pellet surface separating the pellet interior from the surrounding ablated material is explicitely resolved as well as the

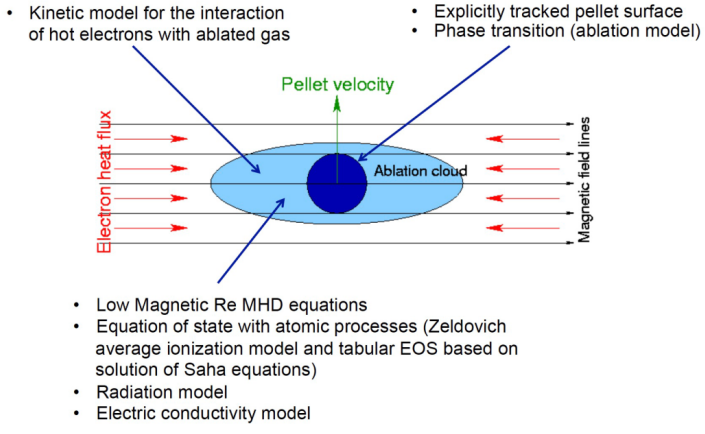

Figure 1: *schematic of physics models*

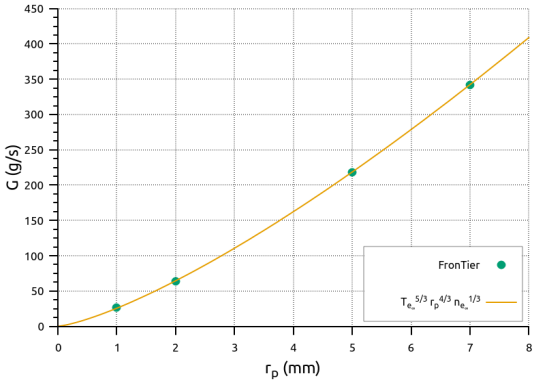

(a) $T_{e_\infty} = 2\,\mathrm{keV}, \quad n_{e_\infty} = 10^{14}/\mathrm{cc}$ (b) $r_p = 2\,\mathrm{mm}, \quad n_{e_\infty} = 10^{14}/\mathrm{cc}$

Figure 2: *Scaling laws for the ablation rate G.*

Case	r* (mm)	T* (eV)	P* (b)
Semi-analytic	5.95	6.19	6.10
FronTier	5.93	6.21	6.09

(a) *Sonic radius and sonic quantities ($r_p = 2$ mm)*

Case	r_p = 1 mm	r_p = 2 mm	r_p = 5 mm	r_p = 7 mm
Semi-analytic	25.57	64.44	218.6	342.4
FronTier	26.07	64.15	217.7	342.4

(b) *Ablation rate (g/s) for different pellet radii*

Figure 3: *Comparison at fixed plasma temperature $T_{e_\infty} = 2\,keV$ and density $n_{e_\infty} = 10^{14}/cc$.*

boundary between the ablation cloud and background tokamak plasma. The boundary condition at the pellet surface is obtained from the surface ablation model and the cloud-plasma interface is treated as a contact discontinuity. One improvement compared to previous studies [2] is the use of high order WENO scheme with second order flux reconstruction and the explicit interface tracking at the cloud/plasma boundary. This allows for better resolution of the shear flow at the contact discontinuity separating the two fluids.

A new spherically symmetric semi-analytic model for the ablation rate of light-element pellets using a new kinetic-based electron heat flux model [4] was compared with FronTier simulations of neon pellets in 1-D spherically symmetric geometry. Remarkable agreement is found in the ablation rates and the sonic quantities as displayed in Fig. 3. Both models obey approximate scaling laws (Fig. 2) similar to the ones found for hydrogenic pellets [5].

In the spherically symmetric case, the reduction of the ablation rate due to multiple ionization in the ablation flow has little effect on the ablation rate. This is because the first ionization energy of neon is quite high ~ 21 eV compared to deuterium dissociation energies $\sim$ 2.2 eV. Neutrals therefore begin to ionize at distances much further from the pellet than dissociation of molecules in the case of deuterium. Hence atomic processes have a lesser effect on neon ablation rates unless plasma densities are quite large. Note that in Fig. 4 and 5 an earlier version of the

$n_{e\infty} = 10^{14}$ /cc	$T_{e\infty} = 2$ keV	$T_{e\infty} = 5$ keV
$r_p = 2$ mm	52.33 g/s	248 g/s
$r_p = 5$ mm	181 g/s	834 g/s

$n_{e\infty} = 10^{14}$ /cc	$T_{e\infty} = 2$ keV	$T_{e\infty} = 5$ keV
$r_p = 2$ mm	53.5 g/s (+2.2%)	254 g/s (+2.4%)
$r_p = 5$ mm	178 g/s (-1.6%)	851 g/s (+2%)

Figure 4: *Indicated in parentheses is the relative change in the ablation rate. For the above plasma and pellet parameters this change is negligible. Left: ideal case, no ionization. Right: ionization allowed.*

$n_{e\infty} = 4x10^{14}$ /cc	$T_{e\infty} = 2$ keV	$T_{e\infty} = 5$ keV
$r_p = 2$ mm	127 g/s	582 g/s
$r_p = 5$ mm	439 g/s	2033 g/s

$n_{e\infty} = 4x10^{14}$ /cc	$T_{e\infty} = 2$ keV	$T_{e\infty} = 5$ keV
$r_p = 2$ mm	110 g/s (-13.4%)	356 g/s (-38.8%)
$r_p = 5$ mm	334 g/s (-24%)	1629 g/s (-20%)

Figure 5: *At higher plasma parameters and pellet radius, the effects of atomic processes on the ablation rate become significant. Left: ideal case, no ionization. Right: ionization allowed.*

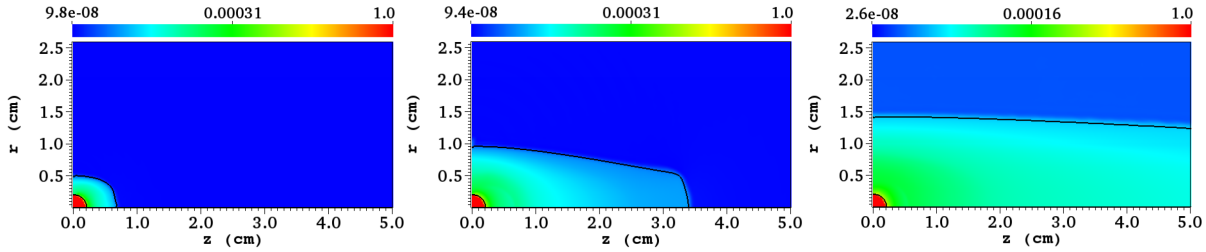

(a) $t = 1\mu$sec (b) $t = 3\mu$sec (c) $t = 10\mu$sec

Figure 6: *Cloud expension in 2T magnetic field at early times. Pictured: the mass density.*

kinetic model is used, slightly different from the revised model of [4]. This does not change the trend observed in these figures.

Influence of the electronic directional heating along the field lines and $J \times B$ force on the ablation flow are studied in 2-D axisymmetric geometry. Ionization of the cloud due to electronic heating channels the flow along the magnetic field lines leading to stronger shielding compared to the isotropic flow expansion that occurs in the spherically symmetric model.

Unless noted otherwise the following pellet radius and plasma parameters were used for the simulations: $r_p = 2$ mm, $T_{e\infty} = 2$ keV, $n_{e\infty} = 10^{14}$ /cc. The width of the ablation channel contracts with increasing B field strength. This in turn leads to stronger shielding and reduces steady state ablation rates (Fig. 7). The channel squeezing and sharp drop in the density gradient at the cloud edge is seen in Fig. 10 for $B = 2T$ and $B = 9T$. The cloud pressure decreases to the pressure of the tokamak plasma at the cloud boundary corre-

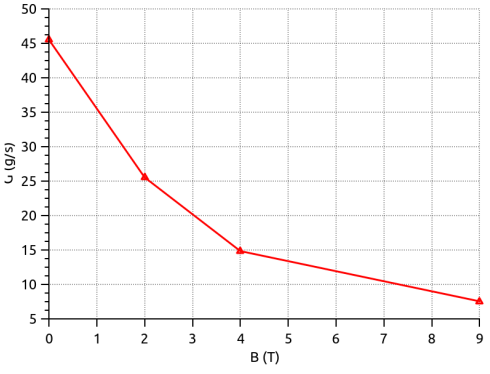

Figure 7: *Steady state ablation rates in increasing B field strengths.*

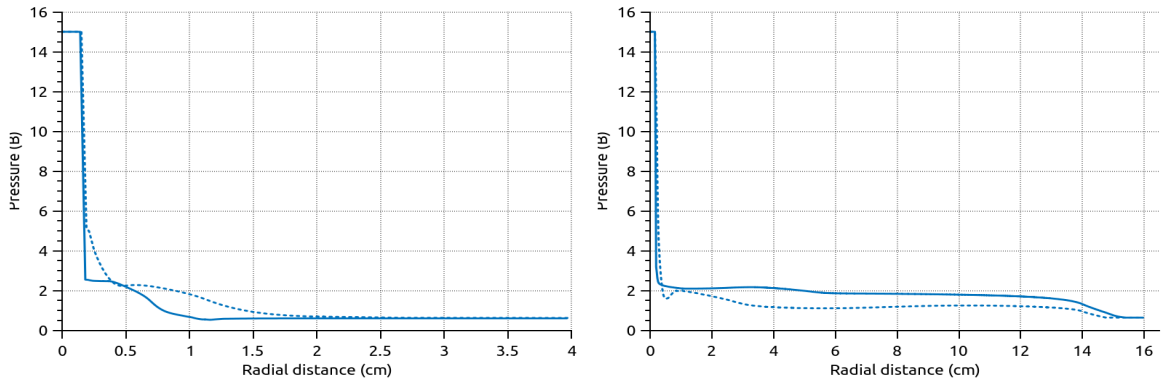

(a) $z = 0$ cm (b) $r = 0$ cm

Figure 8: *Pressure profiles along the z = 0 cm plane (*a) and r = 0 cm plane (b) for B=2T (dashed line) and B=9T (solid line).

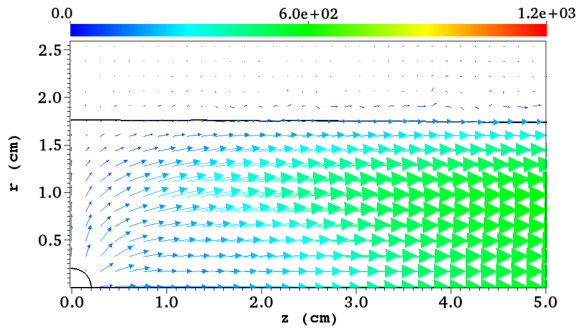

Figure 9: *Velocity flow field (cm/ms). Interface tracking at the cloud boundary captures the tangential velocity discontinuity of the two media.*

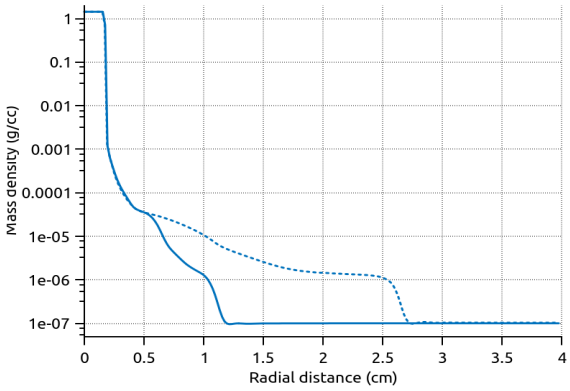

Figure 10: *Mass density distribution along the mid-plane z = 0 cm. Dashed line 2T, solid line 9T.*

sponding to the contact discontinuity (Fig. 8, a). The same boundary condition was proposed in [6] for hydrogen pellets where it was also shown that the channel width decressed with magnetic field strength in qualitative agreement with FronTier.

Acknowledgment This research has been supported by the US Department of Energy grant SciDAC Center for Tokamak Transient Simulations.

References

[1] D. Shiraki et al., Physics of Plasmas **23**, 6 (2016)

[2] R. Samulyak, T. Lu, P.B. Parks, Nuclear Fusion **47**, 2 (2007)

[3] J. Glimm, J. Grove, Y. Zhang, SIAM Journal on Scientific Computing **24**, 1 (2002)

[4] P.B Parks, "The ablation rate of light-element pellets with a kinetic treatment for penetration of plasma electrons through the ablation cloud", submitted to Physics of Plasma

[5] P.B. Parks, R.J. Turnbull, Physics of Fluids **21**, 1 (1978)

[6] P.B. Parks, Nuclear Fusion **31**, 1431 (1991)

[7] R. Ishizaki, P.B. Parks, N. Nakajima, M. Okamoto, Physics of plasma **11**, 8 (2004)